14th International Conference on Pressure Vessel Technology

Fracture of Cylindrical Shells Subjected to Internal Explosion: Numerical Simulation

Y. Du[a],*, L. Ma[a], J.Y. Zheng[a,b,c]

[a]*Institute of Process Equipment, Zhejiang University, Hangzhou 310027, China*
[b]*The State Key Laboratory of Fluid Power Transmission and Control, Zhejiang University, Hangzhou 310027, China*
[c]*High-pressure process equipment and safety engineering research center of ministry of education, Zhejiang University, Hangzhou 310027, China*

Abstract

Coupled analysis of explosion-driven fracture is a challenging task due to complicated fluid-structure interactions (FSI) and local large deformations. In this paper, a coupled Finite Element Method-Smoothed Particle Hydrodynamics (FEM-SPH) method was proposed to simulate the fracture of cylindrical shell subjected to internal explosion. The cylindrical shell was modeled by FEM and the movement of detonation products was modeled by SPH, where they were coupled by penalty contact algorithm. A rate-dependent failure criterion for steels at high strain rate conditions was employed in the simulation, which was presented and verified in our previous work. Results showed the interaction between blast wave and cylindrical shell, the dynamic crack propagation and the finial fracture morphology of cylindrical shell. The decoupled analysis was also conducted to make a comparison. It is found the coupled FEM-SPH method can well handle the complicated FSI problem which including local large deformations and ruptures. Compared with decoupled analysis, the fracture of coupled FEM-SPH analysis shows a better agreement with experimental results. In addition, though the over-predicted explosive loads in decoupled analysis cause a severer bulging deformation of cylindrical shell, but the finial fracture is smaller than that of coupled FEM-SPH analysis.

* Corresponding author. Tel.: 86-571-87953393; fax: 86-571-87953393.
   E-mail address: du.yang.0918@163.com

1. Introduction

Explosion-driven fracture of shell structures is often encountered in the chemical, nuclear and transportation industries [1], e.g., pipe rupture at Hamaoka Nuclear Power Plant in Japan [2] (see Fig. 1). It has been of research interest for many years considering the benefits to the analysis of industrial hazards related to explosion and failure-based design of explosion containment vessels (ECVs) [3-5].

Fig. 1. Pipe rupture due to internal explosion at Hamaoka NPP [2].

Besides experimental studies, numerical methods are exploited to describe this physical event. Generally, numerical analyses can be categorized into decoupled and coupled analyses. The decoupled analysis calculates explosive loads as if the structure was rigid and then applies these loads to the failure model of the structure. Examples are Song J H [6,7], Gato C [8] and Liu S J [9]. The shortcoming of this analysis is the calculated explosive loads are often over-predicted, especially if significant motion or failure of the structure occurs during the loading period [10][1]. In a coupled analysis, the explosion process is simulated simultaneously with structural fracture. By considering the interaction between blast wave and structure, the fracture due to explosion can be predicted more accurately. However, because of large deformations, local topology changes and complicated contact algorithms, coupled analysis of explosion-driven fracture is a challenging task and the related literature is quite limited. Cirak F etc. [11] developed a level-set-based fluid-structure coupling approach which was successfully applied in the simulation of the fracture of aluminum tube due to gaseous detonation. But the approach is mainly applicable to thin structures.

Additionally, few studies involve the comparisons of size and shape of fracture obtained by above two types of analyses. Also, the accurate prediction of explosion-driven fracture needs a good knowledge of failure mode and failure criterion of blast-loaded structures.

Smoothed particle hydrodynamics (SPH) is a meshless method and it was initially developed to solve astrophysical problems [12-14]. Because of its adaptive feature, it can naturally handle problems with extremely large deformation [15-17]. However, its computational efficiency and implementation of boundary conditions are still not as good as grid based methods such as Finite Element Method (FEM).

In this paper, a coupled FEM-SPH method was proposed to simulate the fracture of cylindrical shell subjected to internal explosion. The cylindrical shell was modeled by FEM and the movement of detonation products was modeled by SPH, where they were coupled by penalty contact algorithm. A rate-dependent failure criterion for steels at high strain rate conditions was employed in the simulation, which was presented and verified in our previous work. Results showed the interaction between blast wave and cylindrical shell, the dynamic crack propagation and the finial fracture morphology of cylindrical shell. Also, the decoupled analysis was conducted to make a comparison with the coupled FEM-SPH analysis.

2. Numerical model

2.1. Coupled FEM-SPH analysis model

For various explosions that may occur in industries, TNT equivalency method [18] is the most common and widely used method to describe their strengths. Based on the above consideration, the TNT is taken as the explosive material in this paper.

The coupled FEM-SPH analysis model is established based on our previous experiment [19], as shown in Fig. 2. The cylindrical shell and explosive are discretized by finite elements and SPH particles, respectively. The cylindrical shell is made of GB/JB 20 steel (AISI 1020) and its failure mode under blast loading is deeply studied in our previous work [20, 21]. Its inner diameter is 150 mm, the thickness is 18.5 mm, and the length is 1000 mm. To ignite crack propagation, an elliptical crack within a certain size range is set on the middle of the shell as the initial flaw. The two ends of the shell are completely constrained considering the large weights of flanges at the two ends in the experiment. The cylindrical high explosive TNT is located in the center of the shell. The charge weights are 500 g and 745 g considering the fact that the fracture behavior of the cylindrical shell changes greatly under the load of about 600 g TNT [20].
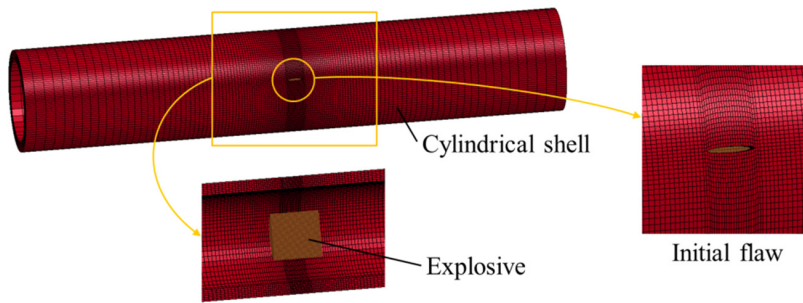

Fig. 2. Coupled FEM-SPH analysis model

The cylindrical shell and explosive are modeled by FEM and SPH respectively considering the complicated FSI and computational efficiency. It is noted the air is not taken into account in the numerical model, for Henrych [22] pointed out the explosion in air can be regarded as the explosion in empty space in the vicinity of explosive charge.

The detonation products of high explosive are described by the following JWL equation of state.

$$p = C_1\left(1 - \frac{\omega}{R_1 V}\right)e^{-R_1 V} + C_2\left(1 - \frac{\omega}{R_2 V}\right)e^{-R_2 V} + \frac{\omega E_0}{V} \tag{1}$$

Where p, V and E_0 are the pressure，relative volume and specific internal energy, respectively. $C_1, C_2, R_1, R_2, \omega$ are constants obtained by experiments. Also, the initial density ρ_0, detonation velocity D and Chapman-Jouget pressure P_{CJ} are involved to start up the computation (see Table 1).

The significant feature of explosively loaded structures is that the strain rate of material is up to 10^1-10^6 s^{-1} [23]. Considering this, a Johnson-Cook type constitutive equation is used for the cylindrical shell.

$$\sigma = \left(\sigma_0 + E_1\varepsilon\right)\left(1 + g\,ln\frac{\dot{\varepsilon}}{\varepsilon_0}\right)\left(1 - \alpha\frac{T}{T_0}\right) \tag{2}$$

Where σ is effective stress, $\dot{\varepsilon}$ is strain rate, and T is material temperature. σ_0, $\dot{\varepsilon}_0$ and T_0 are the reference stress, reference strain rate and reference temperature of the material. E_1, g, and α are the material constants which characterize strain hardening, strain rate hardening and temperature softening. The relating material parameters are given in Table 2.

Metal materials at high strain rate conditions often fail by adiabatic shear mode. Based on above knowledge, a rate-dependent failure criterion was derived from the instability analysis of the above Johnson-Cook type constitutive equation in our previous work [19]. The rate-dependent failure criterion is used to account for the failure of the cylindrical shell in this paper.

$$\left(1 + g\,ln\frac{\dot{\varepsilon}}{\varepsilon_0}\right)\left(A - \frac{\alpha\beta E_1}{T_0\rho c}\varepsilon\right)\left(\frac{\sigma_0}{E_1} + \varepsilon\right) = 1 \tag{3}$$

Where ρ is the mass density and c is the specific heat capacity of the material. β is the transformation coefficient of heat energy and equals 0.9 in this paper. The constant A characterizes the state of adiabatic shear. Fig. 3 gives the failure criterion represented by Eq. (3) where A is 0.93, which indicates the critical strain decreases with increasing strain rate.
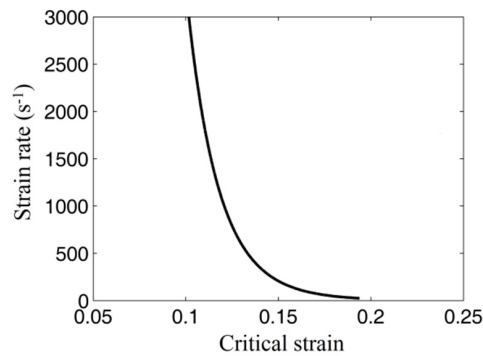

Fig. 3. Rate-dependent failure criterion

Table 1. JWL parameters of TNT.

C_1 (GPa)	C_2 (GPa)	R_1	R_2	ω	E_0 (J/m³)	ρ_0 (kg/m³)	D (m/s)	P_{CJ} (GPa)
371.2	3.231	4.15	0.95	0.30	2.6×10^9	1630	6930	21

Table 2. Material parameters of GB/JB 20 steel.

σ_0 (MPa)	E_1 (MPa)	$\dot{\varepsilon}_0$ (s⁻¹)	g	α/T_0 (K⁻¹)	ρ (kg/m³)	c (J/kg/K)
380	599	1.0×10^3	3.23×10^{-2}	5×10^{-4}	7.85×10^3	470

2.2. Coupling approach

The FEM and SPH are coupled by penalty contact algorithm [24]. In the simulation, it is checked whether any SPH particles penetrate element surfaces at the beginning of every timestep. If no penetration happens, no treatment is needed. Otherwise, contact forces are applied between those element surfaces and SPH particles which satisfy the penetration condition, where the contact force is proportional to the contact stiffness and penetration depth (see Fig. 4). This is equivalent to put a spring between SPH particles and element surfaces to prevent penetration.
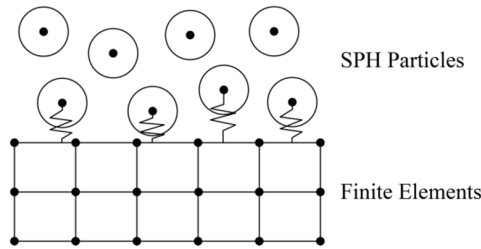
Fig. 4. SPH particles contact with finite elements.

Improper contact stiffness will cause penetration or computational instability due to the significant differences in the stiffness of GB/JB 20 steel and detonation products. In this paper, the contact stiffness is determined based on stability considerations, taking into account timestep and nodal masses. It is calculated by the following formula.

$$k = \max\left(k_1 \frac{Ks^2}{v}, k_2 \frac{m}{\Delta t^2} \right) \tag{4}$$

Where k is contact stiffness. k_1, k_2 are penalty scale factors. K is the material bulk modulus, s is the segment area, v is the element volume, m is the nodal mass and Δt is the global timestep.

2.3. Decoupled analysis model

The decoupled analysis is also conducted in this paper to make a comparison with the coupled FEM-SPH analysis. Firstly, the 1/8 finite element model (see Fig. 5) which consists of cylindrical shell, air and explosive is established to obtain the explosive loads on the inner surface of the cylindrical shell. In this model, the cylindrical shell is described by rigid material model. The air is taken as ideal gas, and the polynomial equation-of-state is used for it with initial density of 1.293 kg/m^3, initial internal energy of 2.53×10^5 J/m^3, and polytropic index of 1.4. The detonation products of high explosive are also described by JWL equation of state [Eq. (1)]. And ALE (Arbitrary Lagrangian-Eulerian) method is used to cope with FSI problem in this finite element analysis.

Then, as shown in Fig. 6, the obtained explosive loads are applied to the failure model of the cylindrical shell which is the same with that in the coupled FEM-SPH analysis to accomplish the decoupled analysis.
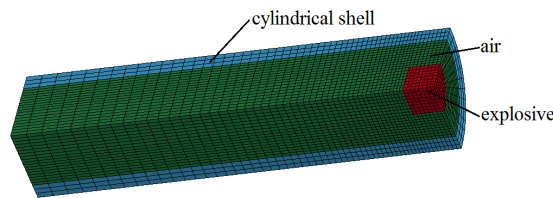

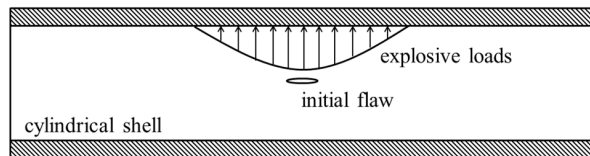Fig. 5. Finite element model to obtain explosive loads.

Fig. 6. Decoupled analysis model.

3. Simulation results

3.1. Blast wave-cylindrical shell interaction

Both the coupled FEM-SPH analysis and the decoupled analysis are accomplished based on the software LS-DYNA. The rate-dependent failure criterion [Eq. (3)] and the contact stiffness calculation formula [Eq. (4)] are employed in the analyses by modifying the keyword file of LS-DYNA. Once the failure condition is satisfied, the corresponding nodes and elements are deleted and thus the crack propagation can be simulated. The penalty scale factors k_1 and k_2 are carefully set in order to keep FEM and SPH well coupled at every timestep.

The interaction between blast wave and cylindrical shell when charging 745 g TNT is given in Fig. 7. As shown, when the explosive is initiated, the blast wave travels outward from the initiation point and then is reflected by the inner surface of the cylindrical shell. As a result, a high stress region forms in the middle part of the cylindrical shell and bulging deformation appears. Also, the crack begins to propagate from the inner wall of the cylindrical shell [see Fig. 7 (b)]. The reflected blast wave then gathers to the centreline of the cylindrical shell and moves to the wall of cylindrical shell again [see Fig. 7 (c)-(f)]. The blast wave will attack the cylindrical shell several times, but the intensity decreases dramatically. One the crack runs through the cylindrical shell, the highly pressurized detonation products violently escape from the fracture and will further promote crack propagation. The phenomenon under the load of 500 g TNT is similar. It can also be seen that the movement of blast wave and fracture of cylindrical shell are well coupled together.
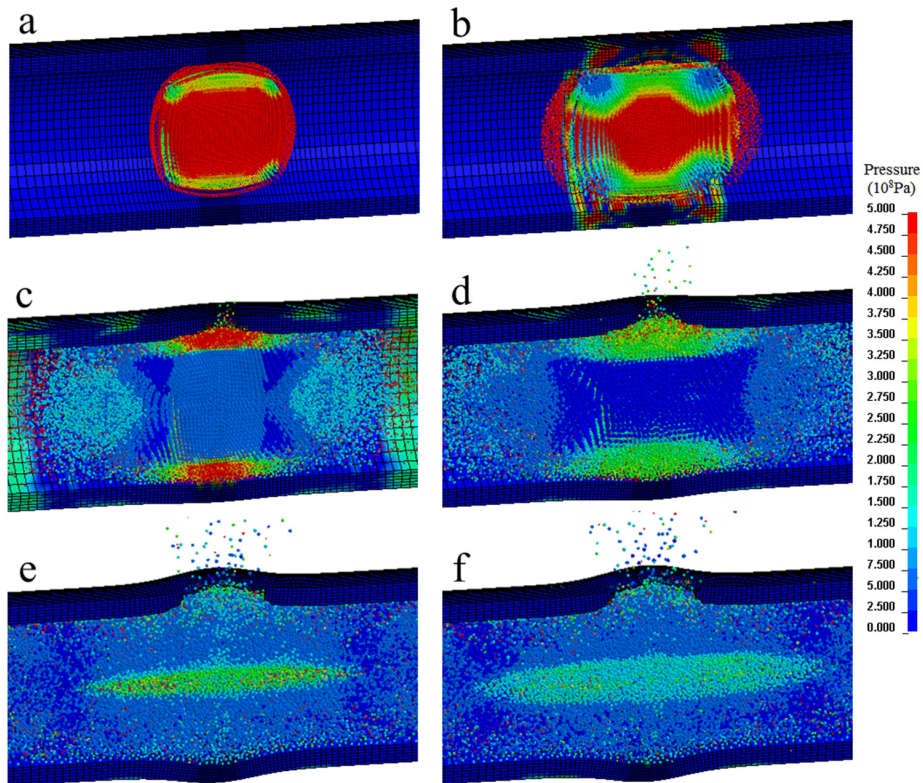

Fig. 7. Blast wave-cylindrical shell interaction: (a) t=13 μs, (b) t=20 μs, (c) t=45 μs, (d) t=60 μs, (e) t=100 μs, (f) t=110 μs.

3.2. Dynamic crack propagation

Figure 8 gives the crack propagation and effective strain under the load of 500 g TNT. As shown, the crack propagates along the axial direction of the cylinder and its finial length is 8.6 cm, where the initial crack length is 3 cm and width is 0.4 cm.

Figure 9 shows the crack propagation and effective strain with the same initial crack, but under the load of 745 g TNT. It is found the crack first run straight for some distance, but then bifurcate along the spiral direction of the cylindrical shell. The finial crack size is obviously larger than that under 500 g TNT and more area of the cylindrical shell deforms plastically. The results are compatible with the conclusion given by Ref [20] that the dynamic fracture behavior of the cylindrical shell changes greatly under the load of about 600 g TNT.
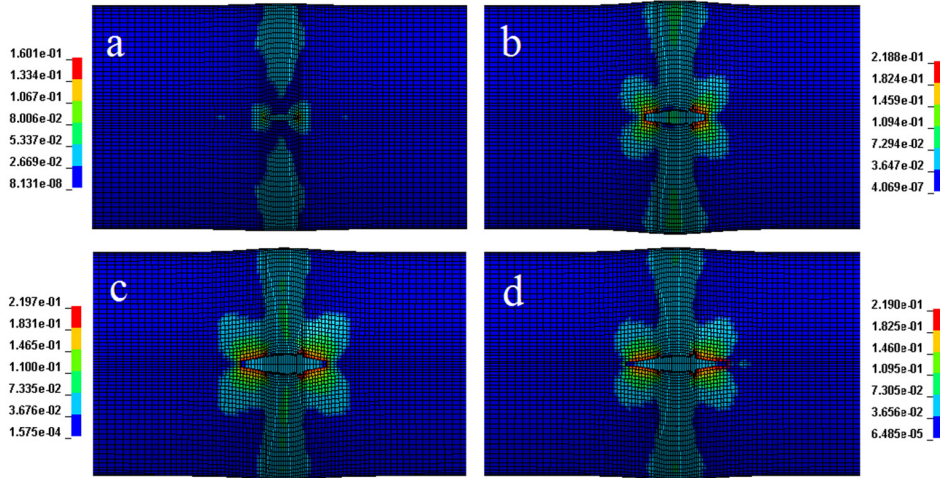

Fig. 8. Crack propagation and effective strain with 500 g TNT: (a) t = 45 μs, (b) t = 80 μs, (c) t = 150 μs, (d) t = 500 μs.
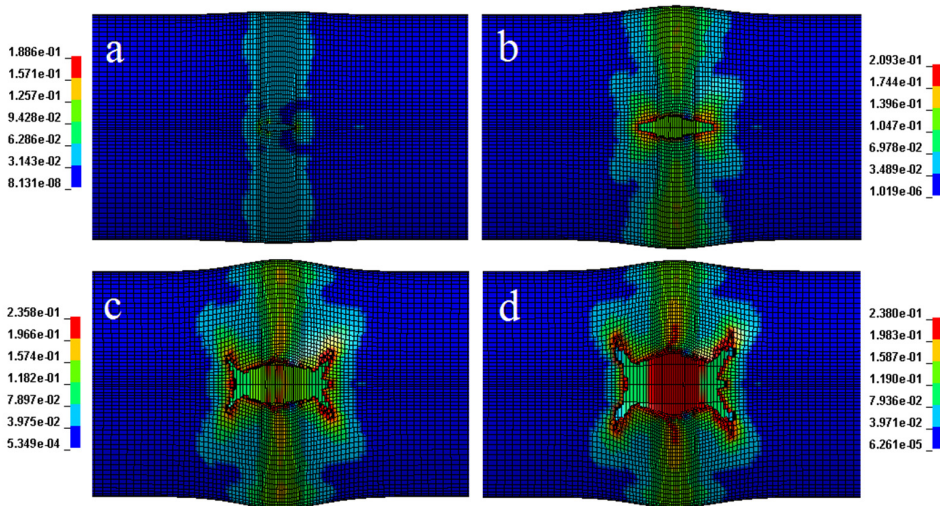
Fig. 9. Crack propagation and effective strain with 745 g TNT: (a) t = 45 μs, (b) t = 80 μs, (c) t = 140 μs, (d) t = 500 μs.

4. Fracture comparison

Figure 10 gives the comparison of fracture morphology from coupled FEM-SPH and decoupled analyses under the load of 500 g TNT. It is found the fracture size of decoupled analysis is smaller than that of coupled FEM-SPH analysis.

Figure 11 shows the comparison of fracture morphology under the load of 745 g TNT. It is also found the fracture size of decoupled analysis is smaller than that of coupled FEM-SPH analysis. It is mainly because when the crack runs through the cylindrical shell in coupled FEM-SPH analysis, the highly pressurized detonation products will release from the crack intensely and enlarge the fracture, which is consistent with the actual situation. Besides, compared with decoupled analysis, the fracture of coupled FEM-SPH analysis shows a better agreement with experimental results. It is noted that the simulated crack length and deformation extent in coupled analysis are smaller than the experimental ones. It can be explained that in the experiment the cylindrical shell has been explosively loaded several times before eventually rupture with 600 g TNT [20].

Figures 12 and 13 give the radial displacement of representative point which located on the outer surface of the cylindrical shell and the opposite side of fracture. It can be concluded that compared with coupled FEM-SPH analysis, the bulging deformation of cylindrical shell in decoupled analysis is severer, which is reasonable considering the over-predicted explosive loads in decoupled analysis.

As for the influence of initial crack size on the finial simulated fracture, our previous work [20] has proved that the finial fracture mainly depends on the load condition and the rate-dependent failure criterion. The initial crack is used to ignite crack propagation. It does not cause obvious difference in the finial fracture.
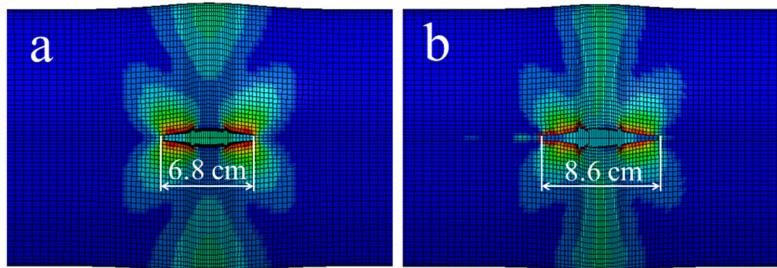

Fig. 10. Fracture comparison with 500 g TNT: (a) decoupled analysis, (b) coupled FEM-SPH analysis.
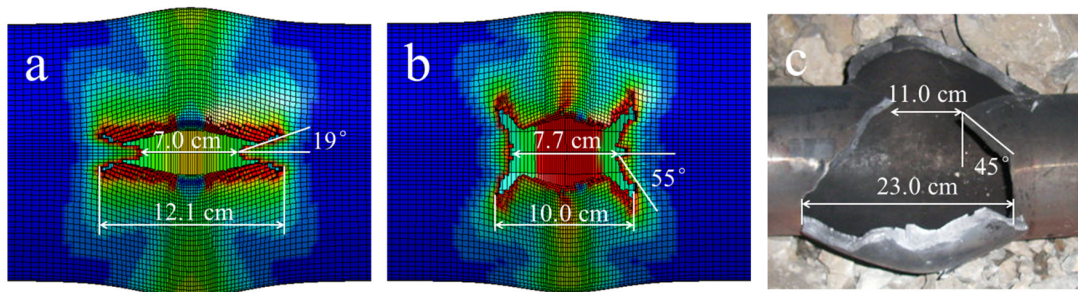

Fig. 11. Fracture comparison: (a) decoupled analysis with 745 g TNT, (b) coupled FEM-SPH analysis with 745 g TNT, (c) experiment with 600 g TNT [20].
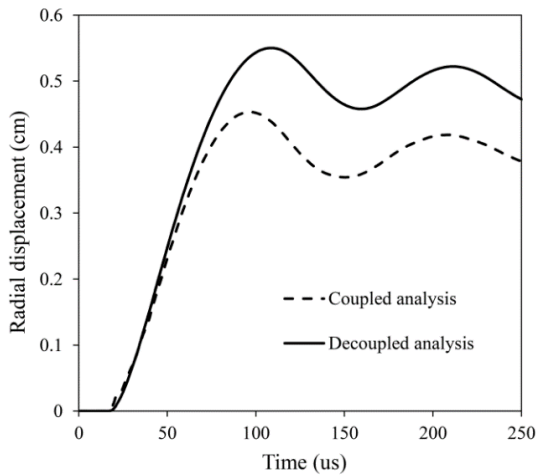
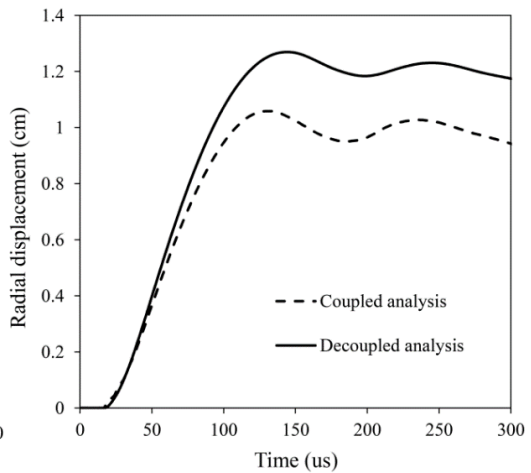Fig. 12. Radial displacement comparison with 500 g TNT

Fig. 13. Radial displacement comparison with 745 g TNT

5. Conclusions

A coupled FEM-SPH method is proposed to simulate the fracture of cylindrical shell subjected to internal explosion. The FEM and SPH are coupled by penalty contact algorithm, where the contact stiffness is determined based on stability considerations, taking into account global timestep and nodal masses. By employing the rate-dependent failure criterion which was proposed in our previous work, the dynamic crack propagation and finial fracture morphology of cylindrical shell are successfully captured.

It is found the coupled FEM-SPH method can well handle the complicated FSI problem which including local large deformations and ruptures. Compared with decoupled analysis, the fracture of coupled FEM-SPH analysis shows a better agreement with experimental results. In addition, though the over-predicted explosive loads in decoupled analysis cause a severer bulging deformation of cylindrical shell, but the finial fracture is smaller than that of coupled FEM-SPH analysis.

Above conclusions can contribute to the analysis of industrial hazards related to explosion and failure-based design of explosion containment vessels.

Acknowledgements

References

[1]   J.E. Shepherd, Structural response of piping to internal gas detonation, Journal of Pressure Vessel Technology. 131.3 (2009) 031204.
[2]   M. Naitoh, F. Kasahara, R. Kubota, et al., Analysis of Pipe Rupture of Steam Condensation Line at Hamoaka-1, (I) Accumulation of Non-condensable Gas in a Pipe, Journal of Nuclear Science and Technology. 40.12 (2003) 1032–1040.
[3]   D. Kim, J.J. Yoh, Predictive model of onset of pipe failure due to a detonation of hydrogen–air and hydrocarbon–air mixtures, International Journal of Hydrogen Energy. 34.3 (2009) 1613-1619.
[4]   T.W. Chao, J.E. Shepherd, Comparison of fracture response of preflawed tubes under internal static and detonation loading, Journal of Pressure Vessel Technology. 126.3 (2004) 345-353.
[5]   T.W. Chao, J.E. Shepherd, Fracture response of externally flawed aluminum cylindrical shells under internal gaseous detonation loading, International Journal of Fracture. 134.1 (2005) 59-90.
[6]   J.H. Song, P. Lea, J. Oswald, Explicit Dynamic Finite Element Method for Predicting Implosion/Explosion Induced Failure of Shell Structures, Mathematical Problems in Engineering. 2013 (2013).

[7]   J.H. Song, T. Belytschko, Dynamic fracture of shells subjected to impulsive loads, Journal of Applied Mechanics. 76.5 (2009) 051301.
[8]   C. Gato, Detonation-driven fracture in thin shell structures: numerical studies, Applied Mathematical Modelling. 34.12 (2010) 3741-3753.
[9]   S.J. Liu, Fracture of thin pipes with SPH shell formulation, International Journal of Computational Methods. 8.03 (2011) 369-395.
[10] T. Ngo, P. Mendis, A. Gupta, et al., Blast loading and blast effects on structures—an overview, Electronic Journal of Structural Engineering. 7 (2007) 76-91.
[11] F. Cirak, R. Deiterding, S.P. Mauch, Large-scale fluid–structure interaction simulation of viscoplastic and fracturing thin-shells subjected to shocks and detonations, Computers & Structures. 85.11 (2007) 1049-1065.
[12] G. R. Liu, M.B. Liu, Smoothed particle hydrodynamics: a meshfree particle method, World Scientific, 2003.
[13] L.B. Lucy, A numerical approach to the testing of the fission hypothesis, The astronomical journal. 82 (1977) 1013-1024.
[14] R. A. Gingold, J. J. Monaghan, Smoothed particle hydrodynamics: theory and application to non-spherical stars, Monthly notices of the royal astronomical society. 181.3 (1977) 375-389.
[15] B. Maurel, A. Combescure, An SPH shell formulation for plasticity and fracture analysis in explicit dynamics, International Journal for Numerical Methods in Engineering. 76.7 (2008) 949-971.
[16] M.B. Liu, G.R. Liu, Z. Zong, et al., Computer simulation of high explosive explosion using smoothed particle hydrodynamics methodology, Computers & Fluids. 32.3 (2003) 305-322.
[17] A.M. Tartakovsky, P. Meakin, Pore scale modeling of immiscible and miscible fluid flows using smoothed particle hydrodynamics, Advances in Water Resources. 29.10 (2006) 1464-1478.
[18] Center for Chemical Process Safety, Guidelines for Chemical Process Quantitative Risk Analysis, Wiley-AIChE, New York, 2000.
[19] L. Ma, Y. Hu, J. Zheng, et al., Failure analysis for cylindrical explosion containment vessels, Engineering Failure Analysis. 17.5 (2010), 1221-1229.
[20] M. Li, H. Yang, D. Yang, et al., Fracture Mode Transition for Explosively Loaded GB/JB 20 Steel Containment Vessels, Journal of Pressure Vessel Technology. 136.3 (2014) 031203.
[21] L. Ma, J. Xin, Y. Hu, et al., Ductile and brittle failure assessment of containment vessels subjected to internal blast loading, International Journal of Impact Engineering. 52 (2013) 28-36.
[22] J. Henrych, R. Major, The dynamics of explosion and its use, Elsevier, Amsterdam, 1979.
[23] K. Kuntiyawichai, F.M. Burdekin, Engineering assessment of cracked structures subjected to dynamic loads using fracture mechanics assessment, Engineering Fracture Mechanics. 70.15 (2003) 1991-2014.
[24] J. Campbell, R. Vignjevic, L. Libersky, A contact algorithm for smoothed particle hydrodynamics, Computer Methods in Applied Mechanics and Engineering. 184.1 (2000) 49-65.